https://doi.org/10.5194/egusphere-2026-2719
Preprint. Discussion started: 27 May 2026

The Role of the Atmosphere during the 2023 Antarctic Sea Ice Minimum

Matthew Goodwin[1], Adam Bateson[1], and Jake Aylmer[1]

[1]Centre for Polar Observation and Modelling (CPOM), Department of Meteorology, University of Reading, Reading, UK

Correspondence: Matthew Goodwin (m.goodwin@pgr.reading.ac.uk)

Abstract.

In February 2023, Antarctic sea ice extent reached a record minimum, yet the mechanisms driving this event remain debated. Here we use a coupled ocean–sea ice model (NEMO-SI3) forced by two different atmospheric reanalyses, ERA5 and JRA-55-do, to investigate the drivers of the 2023 minimum and assess the sensitivity of inferred mechanisms to reanalysis choice. Both simulations capture exceptionally low February sea ice extent during the 2022/23 melt season, though neither atmospheric reanalysis reproduces 2023 as a record minimum, with JRA-55-do showing closer agreement with observations. Substantial regional differences emerge between the two simulations in February 2023: JRA-55-do produces greater sea ice coverage in the Amundsen–Bellingshausen and Ross sectors, while ERA5 yields higher concentrations in the Weddell and Indian Ocean sectors. We further investigate the atmospheric differences between the atmospheric reanalyses - differences in downwelling longwave radiation are the strongest disparity in October, whereas shortwave radiation is the primary disparity in February- suggesting a role for these atmospheric differences in the differing sea ice outcome between the two simulations. Much of the existing literature attributes the 2023 minimum to mechanisms inferred from a single reanalysis, most commonly ERA5. Our results demonstrate that reanalysis choice produces markedly different regional sea ice responses, with implications for the interpretation of both thermodynamic and dynamical drivers. We therefore recommend caution when diagnosing real-world sea ice events from reanalysis-forced simulations and that multiple reanalysis products could be employed to improve the robustness of inferred mechanisms.

1 Introduction

Antarctic Sea Ice is a crucial component of the global climate system. It reflects incoming solar radiation due to its high albedo (Maykut and Perovich, 1987), contributes to ocean bottom water formation (Abernathey et al., 2016), influences weather through atmospheric teleconnections (Hobbs et al., 2016), and acts as a buffer that protects glaciers and floating ice shelves from destructive wave action (Massom et al., 2018), limiting Antarctica's contribution to sea level rise. The sea ice system

https://doi.org/10.5194/egusphere-2026-2719
Preprint. Discussion started: 27 May 2026

is also vitally important for ecosystems and marine life, for instance in acting as a breeding habitat for emperor penguins (Fretwell et al., 2023).

Whilst the Arctic has shown a clear and expected sea ice decline in response to rising global temperatures (Stroeve et al., 2012b; Serreze and Meier, 2018), Antarctic sea ice historically has not followed the same trend, exhibiting a slight increase in extent during the satellite observational record from 1979 to 2014, with maxima recorded in 2012, 2013 and 2014 (Purich and Doddridge, 2023). Since 2015-16 however, this apparent resilience to global warming has given way to a rapid sea ice decline, with major extreme ice loss events in 2022, 2023 (Hobbs et al., 2024; Raphael et al., 2025), 2024 and 2025 (National Snow and Ice Data Center, 2025). On 19 February 2023, a new exceptional minimum Antarctic Sea ice extent (SIE) of 1.77 million square kilometres was observed, 1.02 million square kilometres (36%) less than the 1979- average daily minimum sea ice coverage (Purich and Doddridge, 2023). It has been suggested that the Antarctic sea ice system may have entered a new regime, implying that recent extreme sea ice minima are more than just natural variability (Purich and Doddridge, 2023; Raphael et al., 2025; Diamond et al., 2024; Hobbs et al., 2024). However, there is no clear consensus on the mechanisms behind the 2023 minimum, or relative roles of atmospheric and oceanic drivers.

Antarctic sea ice is influenced by a range of interacting processes, including wind patterns, storms, ocean currents, and air and ocean temperatures. Two main schools of thought have emerged to explain recent Antarctic sea ice decline - subsurface ocean warming, and atmospheric variability and teleconnections (Chan et al., 2025). Recent studies propose a variety of atmospheric mechanisms to explain the exceptional 2023 Antarctic sea ice minimum, with no clear consensus emerging. Some emphasise the role of large-scale modes, such as the Southern Annular Mode (SAM), ENSO-related teleconnections, the Indian Ocean Dipole (IOD), and Zonal Wavenumber 3 (ZW3) wave patterns, which can modulate broad circulation patterns and affect sea ice advection and transport (Wang et al., 2024a; Dou and Zhang, 2025; Wang et al., 2025; Boehm et al., 2025; Ma et al., 2025; Eabry et al., 2024). Others highlight regional circulation anomalies, including deepening of the Amundsen Sea Low or shifts in the Ross and Weddell Sea wind patterns, which can drive localized ice export or ice convergence (Swathi et al., 2025; Mezzina et al., 2024). Radiative factors, such as shortwave and longwave flux anomalies and cloud–radiation feedbacks, have also been implicated in controlling local thermodynamic growth and melt (Boehm et al., 2025; Lenaerts et al., 2017). Finally, events such as storms and cyclones may temporarily enhance ice retreat or slow expansion, influencing the spatial structure of minima (Jena et al., 2024). Others argue that atmospheric anomalies alone are insufficient to explain the magnitude and spatial coherence of the observed decline, instead highlighting oceanic preconditioning and subsurface warming as key contributors to a shift toward a persistently low sea ice state (Purich and Doddridge, 2023; Hobbs et al., 2024; Espinosa et al., 2024; Spira et al., 2026). Several studies further suggest that while large-scale atmospheric modes remain skillful predictors of summer sea ice, the importance of the pre-existing sea ice state has increased in recent years, marking a departure from earlier decades of the satellite record (Hobbs et al., 2024). Together, these contrasting interpretations underscore substantial uncertainty in the relative roles of atmospheric and oceanic processes in driving the 2023 minimum.

https://doi.org/10.5194/egusphere-2026-2719
Preprint. Discussion started: 27 May 2026

Given the scarcity of in situ observations in Antarctica, together with uncertainties in satellite remote sensing of sea ice properties - such as the difficulty in estimating sea ice thickness from radar altimetry, and the high uncertainty in the spatial distribution of sea ice concentration in summer and the marginal ice zone from satellite-derived concentration products(Massonnet et al., 2012; Notz and Marotzke, 2012; Stroeve et al., 2012a), it is challenging to construct a complete and physically consistent picture of the atmosphere–ice–ocean system from observations alone. Atmospheric reanalysis datasets allow the combination of sparse observations with numerical models through data assimilation. These reanalyses are widely used to force sea ice and ocean models, offering a computationally efficient alternative to fully coupled simulations. Although some studies have evaluated reanalysis performance or compared reanalysis products in polar regions, there has been limited investigation of how reanalysis choice affects the interpretation of mechanisms driving the 2023 sea ice minimum.

Tian et al. (2024) found that CMIP6 (Coupled Model Inter-comparison Project 6) simulations of sea ice in the central Arctic align better with satellite observations than the ERA5 reanalysis, which exhibits widespread warm biases exceeding 2 degrees. However an atmospheric reanalysis that performs well for the Arctic does not necessarily perform well for the Antarctic. Wang et al. (2024b) find strong sea ice surface temperature biases in Antarctica, with ERA5 exhibiting the largest warm bias, particularly due to the effect of overestimated cloud simulation. In contrast, for the representation of low level winds in coastal regions, Caton Harrison et al. (2022) finds that ERA5 exhibits the best overall performance, more realistic orography, more realistic jet structure and temperature profile. They indicate that important features of the coastal winds are not well characterised by reanalysis datasets, but with differences between the reanalysis datasets. Tetzner et al. (2019) presents a regional scale evaluation of ERA-Interim and ERA5 reanalyses compared to in-situ observations from 13 automatic weather stations, located in the southern Antarctic Peninsula and Ellsworth Land, Antarctica. They found significant improvement in the performance of ERA5 over ERA-Interim, and that ERA5 is highly accurate at representing the magnitude and variability of near-surface air temperature and wind. However they also found that both reanalyses seem to perform better in the escarpment area (>1000 m above sea level) than on the coast, which has significant implications for the use of the reanalyses to investigate sea ice.

Wang et al. (2016) investigates the performance of reanalysis datasets in reproducing trends in 2m near surface temperature data, comparing NCEP1 (National Centres for Environmental Prediction), NCEP2, ERA-Interim and JRA-55 reanalyses. They found that long term memory was well reproduced, but observational warming/cooling trends in East West Antarctica are not well reproduced; in particular NCEP1, NCEP2 and JRA-55 showed spurious warming trends in many parts of East Antarctica, even in those parts where cooling has been observed. They also found that performance was better on the Antarctic Peninsula where station density is highest. Other reanalysis comparison studies exist, for instance on snowfall (Palerme et al., 2017), precipitation changes (Bromwich et al., 2011), atmospheric behaviour in the Amundsen Sea Embayment (Jones et al., 2016), cyclone tracking (Bromwich et al., 2007) and tropospheric pressure and temperature (Bracegirdle and Marshall, 2012). Orr et al. (2021) investigated differences among four widely used atmospheric reanalysis datasets (ERA5, JRA-55, MERRA-2, and CFSR) in their representation of the dynamical changes induced by springtime polar stratospheric ozone depletion in the Southern Hemisphere from 1980 to 2001. They found that large-scale circulation changes, such as the strengthening of westerly winds in the stratosphere and troposphere and the associated poleward shift of the extratropical jet, are generally consistently represented across all four reanalyses, suggesting that the broad dynamical response to forcing is robust to reanalysis choice. However, the authors also show that differences between reanalyses become more pronounced when examining finer-scale dynamical terms, such as eddy heat and momentum fluxes, wave forcing, and residual circulation. Given that temperature changes, wind forcing, and large scale atmospheric circulation changes have all been implicated as key contributors to the 2023 Antarctic Sea ice minimum, these documented reanalysis differences suggest that inferred mechanisms may be sensitive to the choice of atmospheric forcing.

In this study, we therefore compare simulations forced by two widely used atmospheric reanalyses, ERA5 and JRA-55-do, using a coupled ocean–sea ice model to examine the period leading up to the February 2023 minimum. Whilst previous work has evaluated reanalysis performance against observations of atmospheric variables, our study uses a novel approach, comparing their ability to simulate sea ice extreme events (specifically, the February 2023 minimum) when used as atmospheric forcing for coupled ocean-sea ice models. By analysing differences in simulated sea ice behaviour and associated atmospheric forcing, we assess whether proposed atmospheric mechanisms driving the 2023 minimum are robust across reanalysis products or contingent on reanalysis choice. This has important implications for studies that rely on a single reanalysis dataset to diagnose the drivers of recent Antarctic sea ice extremes.

The rest of this paper is structured as follows: In section 2 we outline the model setup, including the atmospheric reanalyses and observation datasets. In section 3 we present the results of the simulations and analysis, divided into four subsections: trends in Antarctic sea ice compared between observations and model simulations, Sea ice concentration differences between the reanalyses during the 2022/23 melt season, EOF analysis of sea ice variability between model simulations with different atmospheric forcings, and a comparison of atmospheric anomalies in the 2022/23 Melt Season between the reanalyses. Section 4 discusses the results, and Section 5 presents conclusions and summarises the study.

2 Methods

2.1 Model (NEMO-SI3)

We use two coupled NEMO - SI3 (Vancoppenolle et al., 2023) ocean sea ice model simulations. For the model runs, a nominal 2 degree, global, tri-polar ORCA grid is used (giving an approximately regular lon-lat grid in the Southern Ocean region), with a time step of 6 hours. The atmosphere forced runs are initialised in 2009 after a 60-year spinup with climatological forcing (standard NEMO test input). Daily and monthly outputs of key sea ice variables are produced, including concentration, volume, mass fluxes, and atmospheric forcing fields on the model grid. The model setup for this study is similar to the ocean–sea ice component of the latest UK Met Office GC5 global model configuration (Blockley et al., 2024), with some key differences noted below:

https://doi.org/10.5194/egusphere-2026-2719
Preprint. Discussion started: 27 May 2026

1. NEMO version 5.0 (Madec and NEMO System Team, 2024)

2. Activate form drag parameterisation - potentially quite important for Antarctic sea ice processes. Traditional models account for ice-air and ice-ocean drag via a uniform skin drag coefficient, whereas this scheme explicitly represents drag due to discrete obstacles (form drag). Drag coefficients are diagnosed dynamically based on ice-state variables such as ice concentration, ridge area and height, floe draft, and melt pond geometry. This produces varying drag coefficients, which have been shown to better capture sea ice dynamics (Tsamados et al., 2014).

3. Activate topographic melt pond scheme (Flocco et al., 2012) - this is an explicit melt pond parameterisation scheme that represents meltwater accumulation. Melt ponds evolve via realistic processes: input from snow melt, ice melt, and rain, drainage through ice permeability or floe-edge spillover, refreezing, and snow infiltration that modulates radiative effects. This scheme has been shown to enhance realism in simulated summer sea ice evolution.

4. Model is forced with atmospheric reanalysis data rather than using a coupled atmosphere model.

2.2 Atmospheric reanalyses

We use two atmosphere forced simulations - the first is forced by the JRA-55-do atmospheric reanalysis, the second by the ERA5 reanalysis. The JRA-55-do global reanalysis is produced by the Japan Meteorological Agency, spanning 1958 to present. JRA-55-do is an adjusted version of JRA-55 (Tsujino et al., 2018) tailored for driving ocean and sea ice models, using extra independent in situ observations. It is a standard atmospheric forcing for the Ocean Model Intercomparison Project (OMIP) (Griffies, 2016) and uses the 4Dvar advanced data assimilation scheme and high model resolution (55km spatial resolution, 3 hours temporal resolution). Some notable biases persist, including a dry bias in the upper and middle troposphere and in regions of deep convection, unrealistic weakening trends observed in tropical cyclone strength, warm bias in the upper troposphere and cold bias in the lower troposphere, and excess precipitation in the tropics (Kobayashi, Shinya and National Center for Atmospheric Research Staff, 2025). ERA5 is the European Centre for Medium Range Weather Forecasting (ECMWF) reanalysis product (Hersbach et al., 2020). ERA5 provides a globally consistent, high-resolution reanalysis (31 km horizontal, 137 vertical levels) from 1979 to present, with preliminary back-extensions to 1950. The reanalysis integrates a 4D-Var assimilation system with ensemble-derived uncertainty estimates, and offers enhanced forecast skill compared to its predecessor, ERA-Interim. Known biases include: warm biases in the lower stratosphere and tropical upper troposphere, precipitation overestimation in some regions (e.g. in deep convection zones) and snowfall, surface flux uncertainties at high latitudes and warm bias in surface temperature over Arctic sea ice (Hersbach et al., 2020). Both datasets are subsampled to 6 hourly frequency (matching the sea ice model timestep) and interpolated to the ORCA2 grid. The following atmospheric fields are read in to the model:

- Near-surface air temperature (10m for JRA-55-do, 2m for ERA5)
- Near-surface humidity (For JRA-55-do specific humidity, for ERA5 relative humidity)

https://doi.org/10.5194/egusphere-2026-2719
Preprint. Discussion started: 27 May 2026

- Near-surface wind (At 10m for both JRA-55-do and ERA5)
- Mean sea level pressure
- Surface downwelling shortwave/longwave radiation
- Surface total precipitation and snow. For JRA-55-do the total precipiation was calculated offline.

2.3 Satellite observations

In addition to the two atmosphere forced model simulations, two satellite based sea ice observation datasets are used in this study. Both use data from NASA Goddard and NSIDC, based on two different retrieval algorithms, the NASA Team algorithm (DiGirolamo et al., 2022) and the Bootstrap algorithm (Comiso, 2023). Both algorithms offer a long-term (1978 - near present) record, with a consistent algorithm through time (Comiso et al., 1997). Both datasets have a spatial resolution of 25km × 25km and a temporal resolution of 1d. The use of two different observation retrieval algorithms allows the spread between the two observation datasets to be used as an approximation for observational uncertainty. The NASA Team and Bootstrap algorithms both derive sea ice concentration from passive microwave brightness temperatures but differ in methodology. NASA Team uses fixed spectral tie-points and brightness temperature ratios, while Bootstrap uses daily-varying tie-points and scatterplot interpolation. As a result, Bootstrap adapts more dynamically to changing surface conditions, whereas NASA Team is less sensitive to temperature variations but may underestimate thin ice (National Snow and Ice Data Center, 2026). The two observation datasets are interpolated onto the ORCA2 grid before computation of SIE (as the total area where sea ice concentration exceeds 15%). This is consistent with the calculation of SIE within the model which is done online.

https://doi.org/10.5194/egusphere-2026-2719
Preprint. Discussion started: 27 May 2026

3 Results

3.1 Trends in Antarctic sea ice compared between observations and model simulations

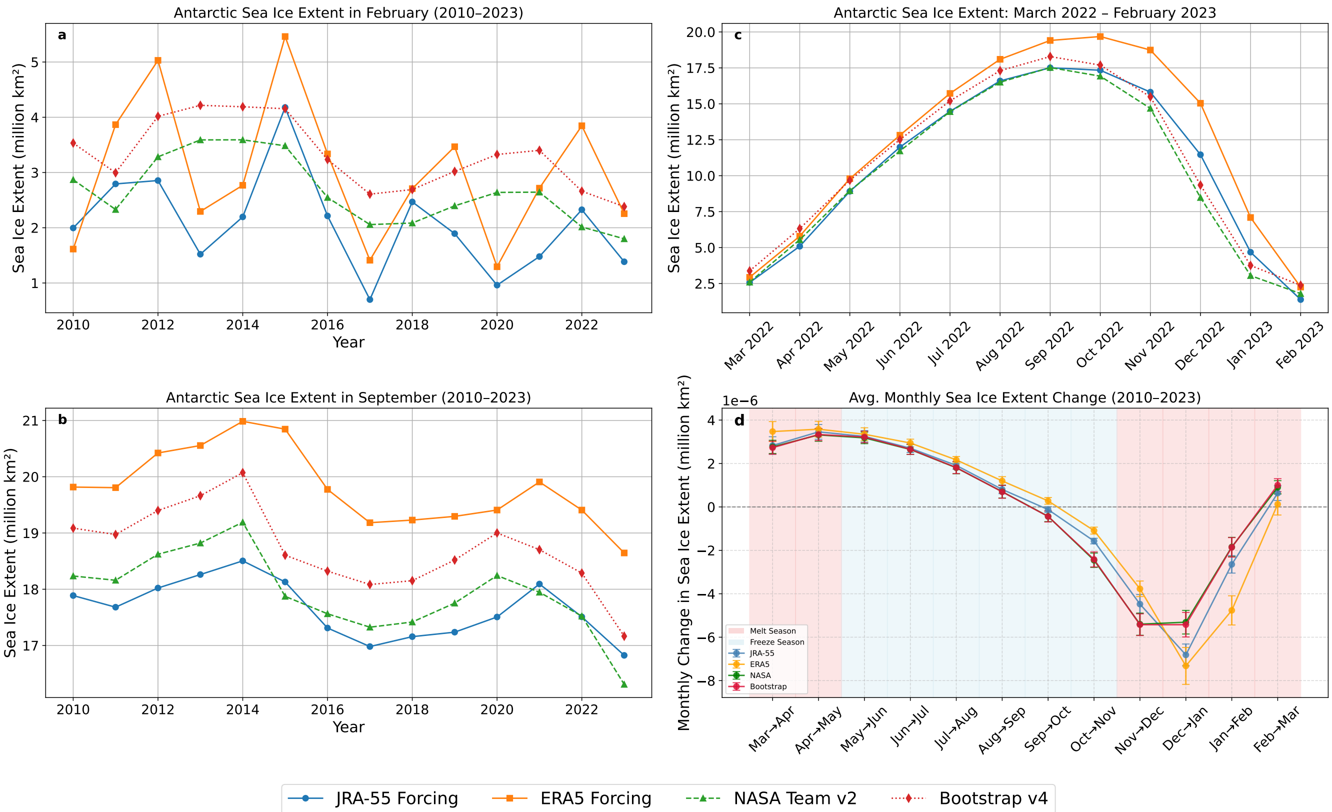

Figure 1. Monthly average Antarctic SIE in February **(a)** and September **(b)** , from 2010-2023, from model simulation output forced by ERA5 or JRA-55 atmospheric reanalysis (orange and blue), and from satellite observations, with two different retrieval algorithms, NASA and Bootstrap (Green and red). **(c)** Monthly average Antarctic SIE from March -Feb 2023. **(d)** Average monthly SIE change, calculated as the difference in monthly average SIE from one month to the next, then averaged over the years 2010-2023. Error bars represent ± 1 standard deviation.

Time series of monthly mean Antarctic SIE (SIE) from 2010–2023 are analysed to compare trends between satellite observations and model simulations forced by atmospheric reanalyses. This comparison assesses the ability of the model simulations to reproduce observed sea ice variability. February and September are selected to represent typical SIE minima and maxima, respectively, isolating the extreme seasonal states from the broader annual cycle (Fig 1, (a) and (b)).

https://doi.org/10.5194/egusphere-2026-2719
Preprint. Discussion started: 27 May 2026

Some aspects of the February SIE are not fully captured by either model forcing, with both simulations exhibiting higher-frequency variability than is evident in the observations, suggesting potential deficiencies in model forcing and/or model physics.

In addition, the models perform poorly in individual years, for example, both simulations produce a sea-ice minimum in 2013, whereas observations indicate a maximum. A comparable divergence occurs in 2020, during which the observed SIE is close to a maximum, but both models produce a minimum. Although the simulated and observed SIE values are consistent in 2023, this agreement should therefore be interpreted with caution, as it may reflect compensating errors rather than robust predictive skill.

The two reanalysis-forced simulations also diverge from each other. The JRA-55–forced run consistently produces lower February SIE relative to ERA5 (except in 2010), and their differences vary greatly over time. In 2012, for example, the ERA5 simulation yields SIE values approximately 70% higher than JRA-55, while the two forcings nearly converge in 2020. Observations indicate that February 2023 was the record-low SIE minimum, yet both model outputs simulate lower minima in 2017 and 2020, failing to capture the timing of the observed extreme. In contrast, the September SIE patterns are more consistent between models and observations. The timing of maxima and minima aligns well, with JRA-55 generally underestimating and ERA5 overestimating SIE. Inter-model differences remain relatively constant throughout the study period. This stability may contradict the hypothesis that the Antarctic sea ice system has entered a new regime, as such a shift might be expected to produce time-evolving divergence among model outputs. Alternatively, it is possible that process driving sea ice system change are either not represented or inadequately represented in the model, or that the cause of the change in Antarctic Sea ice regime may be unrelated to the cause of difference in forced model behaviour, so further investigation is necessary to untangle these processes.

The exaggerated February variability in the reanalysis forced model simulations could arise from the absence of feedbacks between the atmosphere, ocean, and sea ice, which may act to dampen high-frequency variability. This limitation has important implications for studies relying on atmospheric reanalyses. Fully coupled atmosphere–ocean–ice simulations could better represent such feedbacks but are computationally expensive, making the use of prescribed atmospheric forcings a practical alternative. Another possible explanation for the difference in variability is observational uncertainties, particularly during the melt season, when surface melt ponds can complicate satellite retrievals (Aparício et al., 2025). Moreover, using SIE as a diagnostic may obscure key structural changes: extensive regions of thin ice can maintain large SIE values during winter yet melt rapidly in summer. This could provide an alternate explanation for why the September time series reproduces observed variability reasonably well, whereas February simulations diverge markedly. Whilst observations of sea ice thickness could address this, satellite derived observations of sea ice thickness have large uncertainties (Kurtz and Markus, 2012).

Figure 1, panel (c) compares the behaviour of SIE for the observation datasets and two model simulations, in the year leading up to the February 2023 minima. The ERA5 forcing has a later peak (October) than all the other datasets, which peak in

https://doi.org/10.5194/egusphere-2026-2719
Preprint. Discussion started: 27 May 2026

September, although JRA-55 has very similar SIE in both September and October. The freezing period from March up to August is well represented, with good agreement between model output and observations. On the approach to the SIE maxima however, the results of the two atmospheric forcings diverge, with JRA-55 in greater agreement with the satellite observation dataset - this is consistent with the findings of Hobbs et al. (2024). The melting period from September to February 2023 is poorly represented in both model forcings, with both melting at lower rates than observed from October to December, then catching up after December to reach a similar final minima in February 2023.

Examining mean monthly SIE change in Fig 1 (d), the observations and models are relatively close in agreement on the freezing period, with most of the discrepancy in the melting season. The most rapid melting occurs in December-January in both of the two atmospheric forcings, whereas in the observational datasets November-December and December-January have similar SIE melting rates. The transition with the biggest discrepancy between the atmospheric forcings is from January to February. The largest differences in Antarctic SIE (SIE) between simulations forced by the two atmospheric reanalyses occur particularly from October to December , when disparities reach up to approximately $3 \times 10^6\ km^2$ (Fig 1, (c)) This pattern is atypical relative to the 2010–2023 mean (Fig 1, (d)), in which the greatest inter-forcing differences generally occur during the January–February transition. Given that October and November sea ice concentration differences relate to the position of the sea ice edge (Fig 2), this suggests that there were greater differences than usual in simulating the rate of sea ice retreat. The shift in timing suggests that the atmospheric processes driving the differences between ERA5 and JRA-55-do forced simulations in 2022/23 differ from those dominating variability across the longer climatological record.

3.2 Sea ice concentration differences between the reanalyses, focussing on the notable 2022/23 melt season

During September–November , the two model runs show good agreement in sea ice concentration (SIC) across most of the Antarctic domain, with discrepancies largely confined to a narrow coastal ring where SIE differs. In these months, ERA5 consistently produces higher SIE than JRA-55-do across all regions, implying that differences in the forcing datasets exert a largely uniform influence on the sea ice field. By December , however, pronounced regional contrasts emerge. JRA-55 simulates higher SIC relative to ERA5 in the Amundsen, Bellingshausen, and Ross sectors, while ERA5 shows higher SIC in the Weddell and Indian Ocean sectors. Comparison with satellite observations (Fig 3) reveals that both regions of strong model–model contrast correspond to areas where both forcings deviate from observations, indicating that each reanalysis exhibits distinct biases in its representation of atmospheric conditions. Recent sea ice loss has been circumpolar, but particularly pronounced in the Weddell sea (Wu et al., 2025). In Fig 2 the sea ice differences between forced simulations are also significant in the Weddell sea, indicating a likely atmospheric driver for the Weddell sea ice state.

The largest SIC discrepancies between ERA5 and JRA-55 (Fig 2) occur in regions of strong gradients near the sea ice, which is dominated by the position of sea ice edge in the two simulations - plus these differences will also be amplified due to monthly averaging.

https://doi.org/10.5194/egusphere-2026-2719
Preprint. Discussion started: 27 May 2026

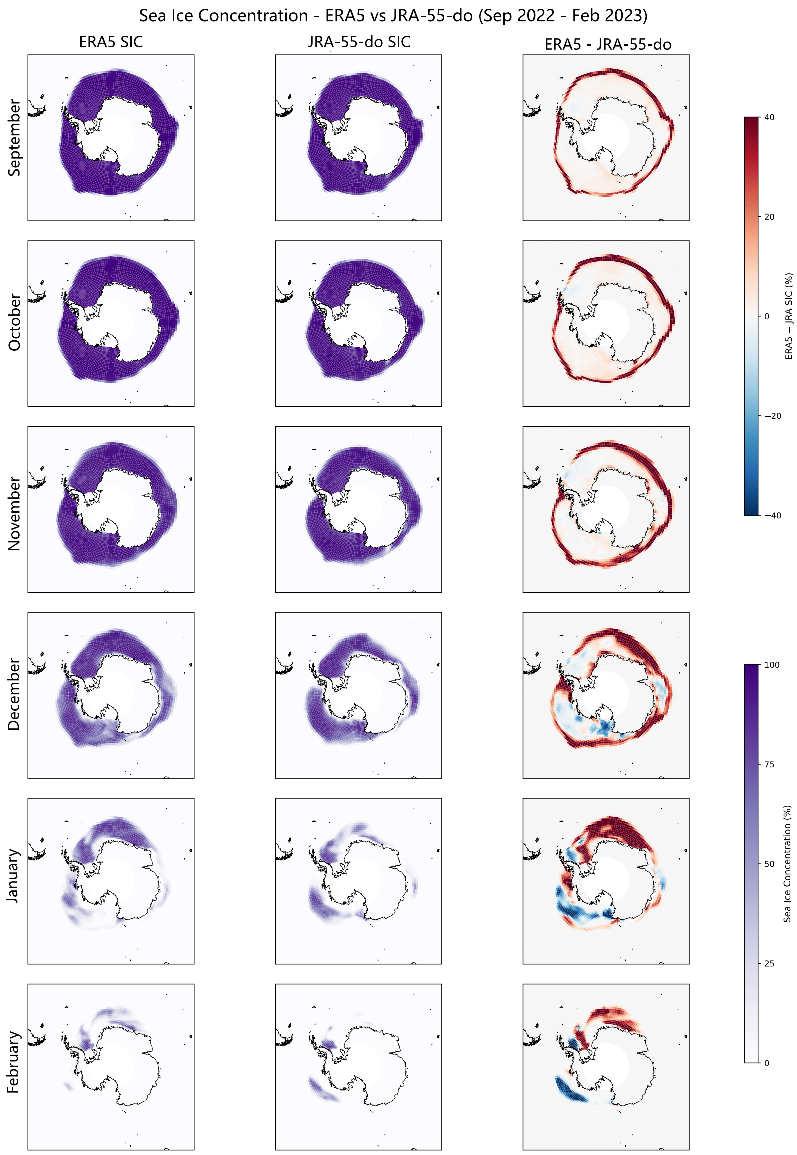

Figure 2. Sea ice concentration plots for JRA-55-do and ERA5 atmospheric forced simulations, from September to February 2023. The third column shows the spatial pattern of sea ice concentration differences between model simulations forced by the two reanalyses. Red regions show where modelled sea ice concentration was higher in the JRA-55-do forced simulation, and vice versa for blue regions.

https://doi.org/10.5194/egusphere-2026-2719
Preprint. Discussion started: 27 May 2026

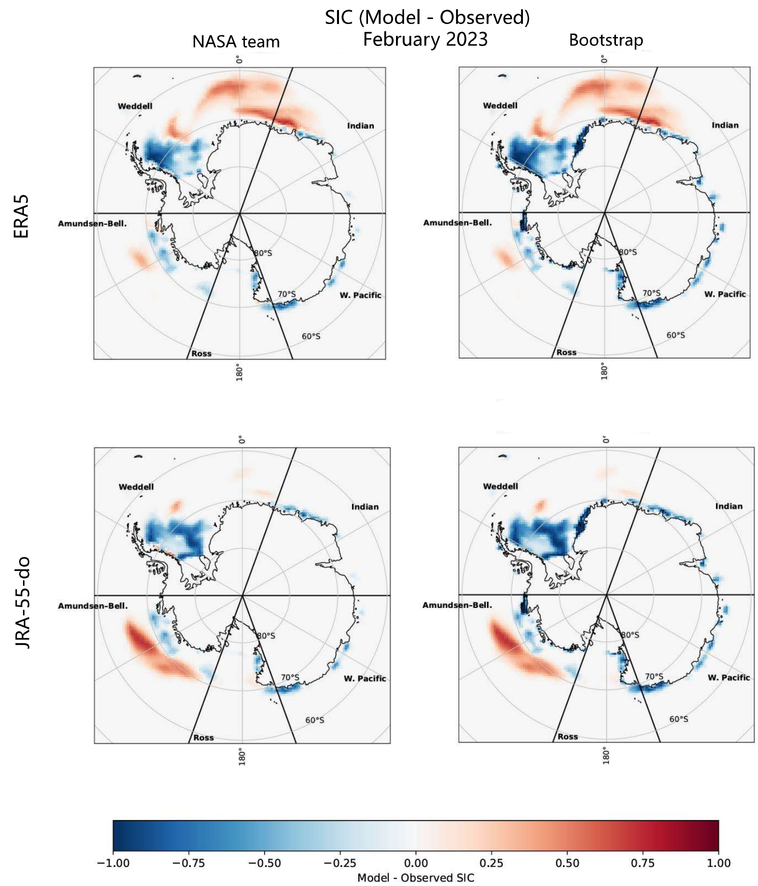

Figure 3. Sea ice concentration difference plots for February 2023. The four panels show difference plots for both JRA-55-do and ERA5 atmospheric forced simulations, compared with two satellite observation retrieval algorithms, NASA and Bootstrap. Red regions show where modelled sea ice concentration was higher in the atmospheric reanalysis forced simulation than observed by satellite, and vice versa for blue regions.

https://doi.org/10.5194/egusphere-2026-2719
Preprint. Discussion started: 27 May 2026

However, spatially uniform differences are also visible away from the ice edge, across the months, but especially prominent in December onwards, indicating systematic thermodynamic differences. These differences (both positive and negative anomalies) are amplified, and visibly grow larger (from top to bottom as time progresses, in Fig. 2), consistent with the action of ice-albedo feedback. This process is reflected in the enhanced melt in the JRA-55-do simulation.

These findings suggest that in these regions, divergent atmospheric conditions, rather than model physics, are responsible for the contrasting sea ice outcomes, given that both simulations use the same coupled ocean–sea ice framework. There is also a role for albedo feedback, i.e. differences being driven by SIC differences itself, although the precise physical mechanisms (shortwave/longwave fluxes, surface air temperature, etc) cannot be determined from these results.

3.3 EOF analysis of sea ice variability between model simulations with different atmospheric forcings

To examine large-scale patterns of atmospheric influence on Antarctic sea ice, Empirical Orthogonal Function (EOF) analysis was applied to monthly Antarctic sea ice concentration (SIC) differences between the ERA5 and JRA-55-do atmosphere forced simulations over 2010–2023. EOF analysis decomposes complex, multi-year variability into a set of linearly independent spatial patterns (statistically distinct modes of variability that cannot be expressed as linear combinations of one another) and their associated temporal coefficients, ranked by the fraction of variance they explain (Lorenz, 1956; von Storch and Zwiers, 1999). EOF analysis has been widely used to characterise sea-ice variability, including to decompose sea-ice concentration fields into dominant spatial modes of variability (Liu et al., 2023; Singarayer and Bamber, 2003), link SIE patterns to the Antarctic Dipole (Yuan and Martinson, 2001), and to explore the relationship between the sea ice system and atmospheric teleconnections (Feng et al., 2019), and for comparative climate model evaluation (Benestad et al., 2023). The analysis was applied to the annual series of each monthly mean separately, in order to minimise the influence of the seasonal cycle and to instead emphasise inter-annual variability. We apply EOF analysis to the difference field of monthly Antarctic sea ice concentration between the ERA5 and JRA-55-do atmosphere forced simulations. This allows us to isolate spatial patterns in the sea ice associated with differences in atmospheric forcing. Applying EOF analysis to the difference field emphasises coherent, large-scale structures in the response, while filtering variability that is shared between the two atmosphere forced simulations. This approach also allows us to link to the February 2023 sea ice anomaly spatial pattern.

Principal components (PCs) are the time series associated with each EOF spatial pattern, and they describe how the amplitude and sign of that pattern varies over time. A positive PC value indicates that the spatial pattern of the corresponding EOF is expressed in the data at that time — so for the EOF of the ERA5 minus JRA-55-do SIC difference field (Figure 4), a positive PC value indicates that ERA5 produces greater sea ice concentration than JRA-55-do in regions where the EOF is positive, and less where it is negative. A negative PC value indicates the reverse. The variance explained by each PC quantifies the fraction of the total dataset variability captured by its corresponding EOF. The first two principal components (PCs) together explain 35% of the total variance, with PC1 accounting for 22.5% and PC2 for 12.5%. EOF1 is characterised by a strong

https://doi.org/10.5194/egusphere-2026-2719
Preprint. Discussion started: 27 May 2026

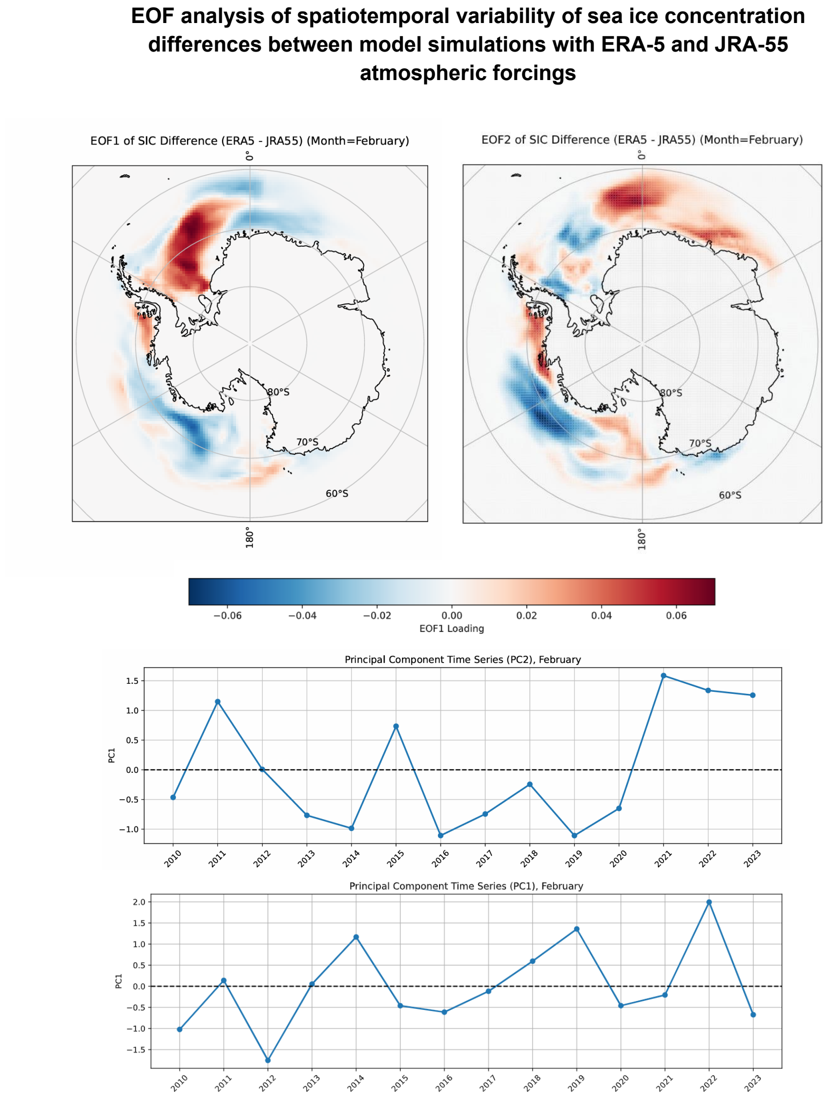

Figure 4. The leading EOF, **EOF1**, represents the dominant pattern of SIC differences between ERA-5 and JRA-55, showing regions where the two reanalyses consistently diverge. Red areas indicate that when PC1 is positive, ERA-5 has higher sea ice concentration than JRA-55. Blue areas indicate that when PC1 is positive, JRA-55 has higher sea ice concentration than ERA-5. The intensity of the color (light to dark) reflects the magnitude of the SIC difference associated with PC1. White or blank areas indicate regions with no significant differences or where the SIC differences are weakly correlated with EOF1. **EOF2**, the second mode, is shown alongside EOF1 and captures a secondary, distinct pattern of SIC differences. **Time Series of PC1 and PC2:** The principal components quantify the temporal evolution of each EOF pattern, showing when and how strongly EOF1 and EOF2 contribute to the SIC differences over time.

https://doi.org/10.5194/egusphere-2026-2719
Preprint. Discussion started: 27 May 2026

positive anomaly in the Weddell Sea and negative anomalies in the northern sea ice edge and Ross Sea, representing a pattern in which ERA5 produces greater sea ice concentration than JRA-55-do in the Weddell Sea and less in the Ross Sea and northern regions when PC1 is positive, with the reverse when PC1 is negative. Both EOF1 and EOF2 represent physically meaningful modes, although neither is dominant. The PC1 time series remains weak during December–February (DJF) 2022/23, while PC2 exhibits a pronounced peak, indicating that the second mode more strongly influenced the 2023 differences between the simulations. The spatial pattern of EOF2 qualitatively corresponds more closely than EOF1 to the February 2023 SIC anomaly pattern, implying that the 2023 differences between ERA5 and JRA-55 are primarily associated with EOF2 rather than the leading mode. Because EOF1 represents the climatologically typical difference pattern, a period of EOF2 dominance suggests that the 2023 differences were atypical and may reflect a distinct atmospheric configuration or physical mechanism. This finding supports the earlier time-series results (Fig 1), which showed that the months of greatest difference between the two model forcings in 2023 deviated from the long-term climatological mean.

Previous studies have identified large-scale wavenumber structures as key patterns of Antarctic sea ice variability. Renwick et al. (2012), for example, found a dominant zonal wavenumber-3 (ZW3) pattern in modelled sea ice variability using EOF analysis. The spatial structure of EOF2 exhibits a similar pattern, with alternating positive and negative SIC anomalies around the Western Antarctic sector, comprising roughly three positive and three negative lobes. This resemblance suggests that differences between the two reanalyses may partly arise from variations in the behaviour of the ZW3 wave pattern. EOF2 displays weak expression over Eastern Antarctica, which aligns with Eabry et al. (2024), who found that ZW3 exerts weaker influence in the East due to the dominance of the Southern Annular Mode (SAM). The EOF2 pattern may therefore reflect a superposition of ZW3 and SAM-related variability. Schroeter et al. (2023) also corroborates these conclusions, finding that the Antarctic sea ice regime shift is associated with the increasingly wave-3-like structure of the Southern Annular Mode, with sea surface temperature anomalies shifting from circumpolar cooling to an asymmetric regional pattern. The pronounced peak in EOF2's PC during February 2023 indicates that this possible combined ZW3–SAM pattern influenced the differences between the ERA5 and JRA-55-do forced simulations during this extreme minimum. This may suggest that sea ice differences between the simulations reflect systematic rather than random divergence in the representation of large-scale atmospheric modes. The ERA-5 forced simulation exhibits higher SIC than JRA-55 in the red lobes of EOF2, whereas the JRA-55 forced simulation has higher SIC in the blue lobes. The dominance of EOF2 in February 2023 highlights that reanalysis choice is critical for interpreting extreme Antarctic sea ice anomalies, as not all reanalyses represent atmospheric variability equally well. In particular, biases in the representation of specific atmospheric modes can lead to systematic over- or underestimation of sea ice concentration in regions where those modes are a primary driver of sea ice variability.

3.4 Atmospheric anomalies in the 2022/23 Melt Season

The following section examines the atmospheric anomalies associated with the 2022/23 melt season. By analysing anomalies in near-surface air temperature, radiative heat fluxes, and surface winds relative to the 2010–2023 climatology, we aim to identify

https://doi.org/10.5194/egusphere-2026-2719
Preprint. Discussion started: 27 May 2026

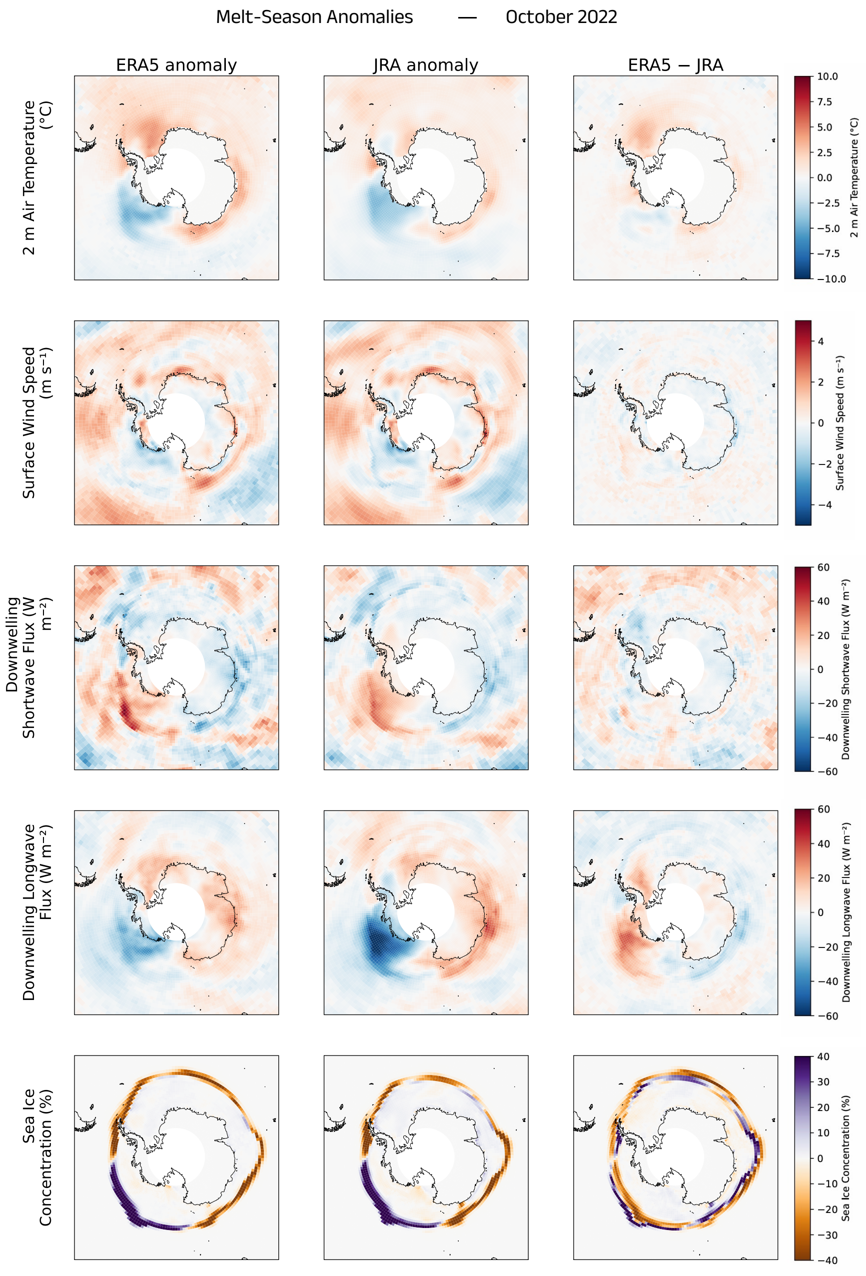

Figure 5. Anomalies in key atmospheric variables (Air temperature, surface wind speed, downwelling longwave flux and short-wave solar heat flux) for October relative to the 2010– climatology. Rows correspond to different variables, while columns represent the ERA5-forced simulation, the JRA-55-forced simulation, and their difference.

https://doi.org/10.5194/egusphere-2026-2719
Preprint. Discussion started: 27 May 2026

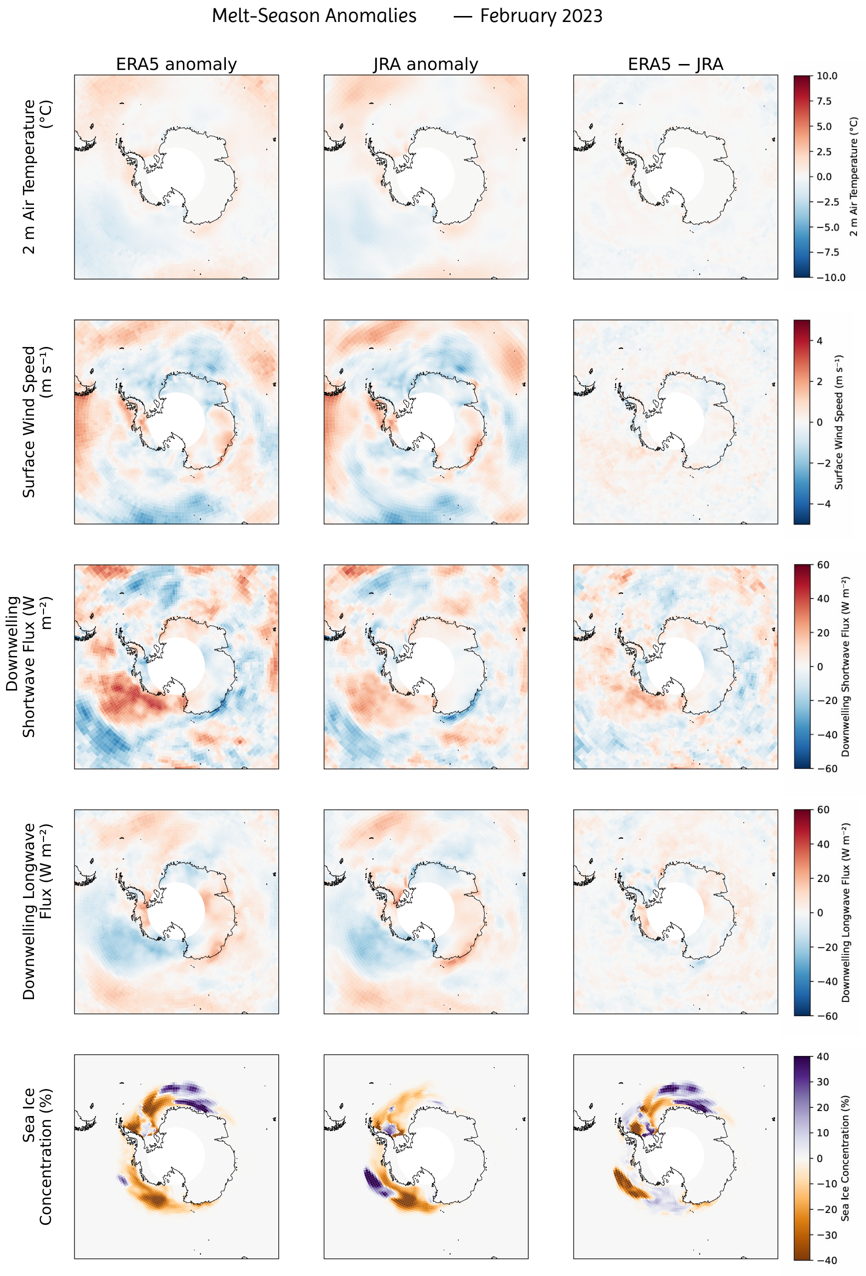

Figure 6. Anomalies in key atmospheric variables (Air temperature, surface wind speed, downwelling longwave flux and short-wave solar heat flux) for February 2023 relative to the 2010–2023 climatology. Rows correspond to different variables, while columns represent the ERA5-forced simulation, the JRA-55-forced simulation, and their difference. The final row also shows sea ice concentration for comparison.

https://doi.org/10.5194/egusphere-2026-2719
Preprint. Discussion started: 27 May 2026

the processes underpinning the regional SIC differences between the reanalyses. Fig. 5 shows anomalies in key atmospheric variables for October relative to the 2010–2023 climatology, as well as differences between these anomalies between the two simulations. Fig. 6 show anomalies for the February 2023 minimum.

Both ERA5 and JRA-55-do forced simulations exhibit cold air temperature anomalies in the Amundsen-Bell region in October, as well as a small region near the Antarctic Peninsula, with warm air temperature anomalies elsewhere. The warm anomaly is up to 5 degrees stronger in the Weddell sea in ERA5 compared with JRA-55-do. A relatively similar pattern in wind speed anomalies is exhibited, with weakened wind speeds in the same Amundsen-Bellingshausen and Antarctic Peninsula regions (up to 4ms^{-1} less) and strengthened wind speeds around East Antarctica. The two reanalyses however are generally consistent over wind speeds, suggesting this might not be a significant cause of differences in sea ice behaviour.

The spatial patterns of downwelling short-wave and long-wave radiation anomalies are also broadly similar, but of opposite sign. Downwelling short-wave flux is solar radiation reaching the surface, which is seasonal (essentially zero in winter due to the polar night) and strongly affected by clouds. Over sea ice, much is reflected due to high albedo, and absorbed by leads and open water. In reanalysis datasets it is very sensitive to cloud representation. October falls within Antarctic spring, as insolation increases following the polar night, with sea ice extent near the typical annual maximum. In contrast, downwelling longwave flux is infrared radiation emitted downward by the atmosphere towards the surface, which is present year-round, and strongly controlled by clouds, water vapour, and temperature. It a major inhibitor of winter ice growth, with warmer, moister air masses leading to more clouds, greatly increasing downwelling longwave flux.

The strongest differences between the reanalyses anomalies in October occur in the down-welling longwave flux. Both have negative anomalies in Amundsen-Bell and the Antarctic Peninsula, and positive anomalies elsewhere, however the negative anomaly is much stronger in JRA-55-do (20-30Wm^{-2} difference), and to a lesser extent the positive anomaly in the West Pacific sector is also around 10-20Wm^{-2} stronger. In contrast, in February (Fig. 6), shortwave radiation anomalies are the strongest source of differences between the reanalyses, suggesting it is possible that they are the driver of differences between the sea ice anomalies in the two simulations. Enhanced short-wave flux directly promotes sea ice melt, and differences in the representation of shortwave radiation between the two reanalysis forcings appear to have led to divergent outcomes in sea ice concentration by February 2023. This behaviour implies clear skies in ERA5 as a potential driver of differences in representation of the February 2023 minimum between the two simulations.

The Amundsen–Bell region exhibits a modest positive sea ice concentration anomaly in October , visible as a narrow band of enhanced SIC in both model simulations, alongside reduced sea ice concentration around much of the remainder of Antarctica. Both positive and negative SIC anomalies are stronger in the ERA5-forced simulation compared with JRA-55-do. In ERA5, SIE in the Amundsen–Bell region is slightly increased, compensated by reduced sea ice concentration closer to the ice edge. This suggests a broadly similar total sea ice state, but with a more spatially diffuse ice edge, while the opposite behaviour is seen elsewhere around Antarctica. The primary atmospheric difference between the simulations is the difference in strength

https://doi.org/10.5194/egusphere-2026-2719
Preprint. Discussion started: 27 May 2026

of the longwave flux anomaly, which spatially corresponds with the regions of largest SIC difference. This is suggestive of a potential role for differences in cloud representation in causing the difference in sea ice edge, given that cloud radiative effects influence surface longwave fluxes. The negative longwave radiation anomaly over the Amundsen Sea could indicate a localized decrease in cloud cover. We cannot rule out other contributing processes without targeted sensitivity experiments, however other studies also suggest a critical role for cloud representation for capturing Antarctic sea ice variability- for instance Alkama et al. (2020) who suggest that cloud radiative effects are capable of dampening the surface energy response to sea ice loss.

In February, near surface air temperature anomalies are weaker in both ERA5 and JRA-55-do. Whilst there are anomalies in both downwelling short-wave and long-wave radiation, the short-wave anomaly is dominant, reaching values of 40-50Wm^{-2} in the Amundsen Bell region. Importantly, this field also exhibits the largest disparity between the reanalyses, identifying it as the primary driver of differences in sea ice concentration between the simulations during the summer minimum.

Together, these results highlight the central role of atmospheric radiative forcing, likely driven by cloud and circulation differences, in shaping Antarctic sea ice variability. They also suggest that additional processes, such as subsurface oceanic variability, may be required to fully explain the magnitude of the 2023 extreme minimum, beyond what can be attributed to atmospheric forcing alone.

4 Discussion

Our study has broader implications for the interpretation of recent literature on the 2023 Antarctic sea ice minimum. Across both simulations, strong wind anomalies in October and February 2023 were consistently represented between ERA5 and JRA-55-do, lending confidence to conclusions that emphasise wind-driven dynamical mechanisms. However, the two reanalyses produced markedly different regional sea ice responses; the Weddell Sea showed the greatest sensitivity to reanalysis choice, with ERA5 forcing producing substantially lower sea ice concentrations than JRA-55-do, while the exceptional loss in the Ross Sea was more robust across both simulations. Thermodynamic fields—particularly downwelling longwave and shortwave radiation—differed substantially between the reanalyses, whereas dynamical fields showed greater agreement. These similarities and differences have direct implications for how conclusions drawn from reanalysis-forced studies should be interpreted. Here, we evaluate whether our results are consistent with mechanisms proposed in the literature to explain the 2023 extreme minimum, and assess the extent to which these mechanisms may be sensitive to the choice of atmospheric reanalysis.

A substantial proportion of the literature relies on a single atmospheric reanalysis—most commonly ERA5—to infer mechanisms driving the 2023 Antarctic sea ice minimum, and our results suggest that some conclusions are sensitive to this choice. Ma et al. (2025) identified a dipole-like pattern of winter sea ice variability across the Bellingshausen, Weddell, and King Haakon VII Seas, termed the East Antarctic Dipole (EAD), which they attributed to thermodynamic and dynamic processes

https://doi.org/10.5194/egusphere-2026-2719
Preprint. Discussion started: 27 May 2026

associated with anomalous low pressure over the Weddell Sea. Atmospheric fields in that study were taken exclusively from ERA5. While we find good agreement between ERA5 and JRA-55-do in wind speed anomalies—suggesting that the associated dynamical forcing is robust—thermodynamic fields differ substantially between the reanalyses. In October, ERA5 exhibits stronger downwelling longwave radiation anomalies in the Weddell Sea and weaker anomalies over East Antarctica compared with JRA-55-do. These differences could amplify thermodynamically driven dipole-like behaviour in ERA5-based analyses, potentially affecting assessments of the strength and spatial structure of the EAD. Similarly, Dou and Zhang (2025) use ERA5 to identify a dipole pattern linked to the co-occurrence of a positive SAM, La Niña, and a negative Indian Ocean Dipole during spring , characterised by increased sea ice in the northern Ross Sea and reduced ice in the Bellingshausen and northern Weddell Seas; however, our simulations reveal considerable sensitivity of regional sea ice behaviour to reanalysis choice in precisely these regions, particularly in the Weddell Sea, where ERA5 forcing produces substantially lower sea ice concentrations than JRA-55-do: suggesting that conclusions regarding the spatial structure of such dipole-like anomalies may be influenced by the atmospheric reanalysis employed.

de Azevedo et al. (2025) likewise use ERA5 and attribute the February 2023 minimum to a positive SAM phase and La Niña conditions during September , which intensified winds and reduced sea ice in the Amundsen, Bellingshausen, and Weddell Seas while increasing ice in the Ross Sea; Jena et al. (2024) further show that storms and cyclones in the Weddell and Ross Seas are likely to have further contributed to the record low conditions, through episodes of exceptional slow ice expansion or even retreat. Our results support the wind-driven component of these interpretations, given the consistency of strong wind anomalies across reanalyses, but the thermodynamic component remains more uncertain. Swathi et al. (2025) uses the ERA5 reanalysis product, as well as ORAS5 ocean reanalysis, and NASA team algorithm for sea ice observations. They found that Weddell Sea and Amundsen-Bellingshausen Sea (ABS) experienced the most decline in austral spring and summer, respectively, while the Ross Sea showed the minimum sea ice loss. They attribute this to lower stratospheric cooling patterns observed during summer, which resulted in a reinforcement of the Southern Annular Mode (SAM), causing intensification of surface temperature inversion, leading to the Antarctic Polar Vortex shifting towards the Equator. The transition from the distinct triple La Niña event to the onset of a warm phase in 2023 resulted in the Amundsen Sea Low (ASL) deepening, which advected warm air into the region and pushed sea ice back towards the coast, reducing its extent particularly in the west of the Antarctic Peninsula region. Similarly, Wang et al. (2024a) link the 2023 summer minimum to a deepened ASL associated with prolonged La Niña conditions. These interpretations differ from our results, which exhibit no pronounced sea ice anomaly west of the Antarctic Peninsula, but instead a notable negative anomaly in the Ross Sea, accompanied by weak near-surface air temperature anomalies. These discrepancies may reflect differences between analyses based on observations paired with reanalysis data and those derived from forced sea ice model output. In contrast, Mezzina et al. (2024), using an ERA5-forced NEMO–LIM configuration, identify the Ross and Weddell Seas as the dominant contributors to summer minima, with thermodynamic processes outweighing dynamic ones at large scales. Whilst our results agree on the exceptional loss in the Ross Sea, the Weddell Sea response is more sensitive to reanalysis choice, with ERA5 forcing producing reduced ice concentrations relative to JRA-55-do. Stronger

https://doi.org/10.5194/egusphere-2026-2719
Preprint. Discussion started: 27 May 2026

shortwave flux anomalies in the Ross Sea under ERA5 further suggest that reliance on a single reanalysis may overemphasise thermodynamic mechanisms at the expense of dynamical contributions.

Richaud et al. (2026), also using a NEMO-SI3 configuration forced by ERA5, investigates the sea ice mass budget during sea ice lows and find that reduced basal growth characterised the 2023 minimum, driven primarily by ocean conditions at the sea ice–ocean interface. They further find an increased importance of dynamics in the sea ice mass budget; since our results show that wind speeds are largely consistent between reanalyses, this lends some confidence to their dynamical conclusions. However, we find that downwelling longwave flux is stronger in JRA-55-do than ERA5 during October , suggesting that the use of ERA5 alone could underestimate the role of surface thermodynamic conditions relative to basal mass budget terms. Kusahara and Tatebe (2025) use a sea ice–ocean model forced exclusively by ERA5 surface boundary conditions to investigate the broader 2016–2023 Antarctic sea ice decline, rather than focusing specifically on the 2023 minimum. Their numerical experiments reveal that thermodynamic boundary conditions—particularly increased sub-polar sea surface temperatures north of the sea ice edge—are the dominant drivers of the decline, with wind stress playing a secondary role. However, since their model relies exclusively on ERA5 forcing, and our results show that thermodynamic fields differ substantially between ERA5 and JRA-55-do, the magnitude and spatial structure of the SST-driven signal in their study may be sensitive to reanalysis choice, particularly in regions such as the Weddell Sea where our simulations show the greatest thermodynamically-driven differences in sea ice response. Goosse et al. (2025) similarly use ERA5 forcing in a NEMO-SI3 configuration, but with a focus on the mean-state relationship between Antarctic Circumpolar Current (ACC) frontal positions and the climatological winter sea ice edge rather than on interannual variability or the 2023 event specifically. They find that the latitude of all ACC fronts correlates strongly (above 0.85) with the mean winter ice edge position, with the Polar Front identified as the most consistent indicator, and attribute this relationship to heat transport via mesoscale eddies and atmospheric processes downstream of major bathymetric features. Since both the atmospheric fields and the NEMO simulation derived oceanic heat fluxes in their study are ERA5-forced, both components of this mechanism could be sensitive to reanalysis choice — our results show that ERA5 and JRA-55-do produce notably different thermodynamic fields and mean sea ice edge positions, suggesting that the relative contributions of oceanic and atmospheric heat transport to the ice edge position in Goosse et al. (2025) may differ under alternative reanalysis forcing. Our study thus highlights that reanalysis sensitivity extends beyond interannual variability and event attribution, and may also affect conclusions about the mean-state processes governing Antarctic sea ice, underscoring the scope of impact from potential biases introduced by using a singular reanalysis product.

Not all relevant studies focus on the causes of the 2023 minimum; some instead examine its consequences or longer-term context, yet still rely on reanalysis forcing, so our results have implications for these too. Josey et al. (2024), using both ERA5 and MERRA-2, investigate not the causes of the 2023 minimum but rather its consequences for ocean–atmosphere interaction, a complementary focus to our study. They find that the strongest ice-retraction regions, located primarily in the Weddell, Bellingshausen and Ross Seas, provided an important new source of turbulent ocean heat loss, with ice concentration reduced by up to 80% and an unprecedented doubling of mid-winter ocean heat loss. Crucially, they find close similarity in the pattern of net heat-flux anomaly between ERA5 and MERRA-2, suggesting that in this case, the intensity of the ocean heat lost

https://doi.org/10.5194/egusphere-2026-2719
Preprint. Discussion started: 27 May 2026

dominates any variations that may arise from differences in reanalysis physics and data assimilation. However, we find whilst there is strong sea ice retreat in the Ross Sea in both JRA-55-do and ERA-5 forced simulations, the two simulations diverge on whether there is more remaining ice in Bellingshausen or Weddell Sea and Indian Ocean.

Atmosphere forced simulations are computationally cheaper than fully coupled climate simulations, and can compensate for sparse in situ observations in the Antarctic. However, even where multiple reanalyses are employed, atmosphere forced simulations still carry additional limitations that warrant consideration. The absence of a coupled atmosphere means that feedbacks between the ocean, sea ice, and overlying atmosphere cannot be captured; Espinosa et al. (2024) demonstrate using a fully coupled Earth system model with nudged winds, that roughly 70% of the 2023 anomaly is attributable to pre-existing Southern Ocean warming, with the remaining 30% linked to atmospheric circulation including a strong zonal wave-3 pattern. Our results show that differences in sea ice behaviour between the simulations are qualitatively consistent with a wave-3-like structure, suggesting that this crucial aspect could itself be influenced by reanalysis choice, as well as the use of reanalysis forced simulations over fully-coupled simulations more generally.

A further limitation, even when using multiple reanalyses, is the high sensitivity of the sea ice system to aspects of reanalyses with a high uncertainty, such as the representation of clouds and radiative fluxes, which are known to be uncertain in reanalysis products. Boehm et al. (2025) attribute a substantial fraction of the decadal decline in Antarctic sea ice to SAM-associated clear-sky shortwave feedbacks, deliberately using satellite observations from CERES rather than reanalysis radiative fluxes, citing known uncertainties in the latter - for instance, moisture and energy budgets in ERA5 experience spurious trends (Mayer et al., 2021) and ERA5 has been shown to have biases in mixed-phase clouds that could impact radiative fluxes (Silber et al., 2019; Lenaerts et al., 2017). Whilst Boehm et al. (2025) finds comparatively weak contributions from longwave radiation, in our simulations, notable differences in longwave radiation anomalies are evident between ERA5 and JRA-55-do, showing an influence of reanalysis choice on anomaly strength. Together, these results suggest that caution is warranted when attributing Antarctic sea ice variability to specific radiative mechanisms based on reanalysis forcing, particularly in regions and seasons where cloud–radiation interactions play a significant role.

5 Conclusions

In this study, we used a coupled ocean sea ice model (NEMO-SI3), forced by two different atmospheric reanalyses, ERA5 and JRA-55-do, to investigate the atmospheric drivers of the February 2023 Antarctic sea ice minimum. By comparing differences in simulated sea ice behaviour and the associated atmospheric conditions, we assessed the sensitivity of interpretations of the 2023 minimum and inferred mechanisms to reanalysis choice.

Our main findings are as follows:

https://doi.org/10.5194/egusphere-2026-2719
Preprint. Discussion started: 27 May 2026

1. The JRA-55-do forced simulation more closely replicates the minimum than ERA-5, highlighting the importance of choice of atmospheric reanalysis.

2. During the 2022/23 summer melt season, both reanalysis-forced simulations capture the exceptionally low February SIE, however, in neither simulation is 2023 a record minimum.

3. Substantial regional differences are evident in the spatial distribution of the remaining sea ice. Relative to ERA5 forcing, the JRA-55-do simulation exhibits increased sea ice in the Amundsen–Bellingshausen and Ross sectors, while ERA5 shows higher sea ice concentrations in the Weddell and Indian Ocean sectors.

4. In October, differences in downwelling longwave radiation emerge as the primary atmospheric disparity, suggesting a role in the differences in sea ice distribution between simulations forced by JRA-55-do and ERA5. In contrast, during February, downwelling shortwave radiation is the most prominent difference between the two atmospheric reanalyses, possibly indicating a more important role in this part of the melt season in shaping sea ice differences.

5. The largest differences in sea ice concentration between ERA5 and JRA-55 forced simulations occur near the ice edge, but as the season progresses, systematic anomalies also develop away from the edge. This amplification of both positive and negative anomalies is consistent with ice–albedo feedback, where initial differences in ice cover alter surface albedo, enhancing melt or growth and reinforcing spatially coherent differences.

6. Surface wind speed anomalies show strong agreement between ERA5 and JRA-55-do, as well as marked departures from climatological conditions, implying that wind-driven mechanisms influencing sea ice variability may be comparatively robust to the choice of atmospheric reanalysis.

7. February sea ice interannual variability is higher frequency in the atmosphere-forced coupled ocean–sea ice simulations than in observations, potentially indicating missing or inadequately represented atmospheric feedbacks that lead the simulations to diverge from observed behaviour. In contrast, interannual variability in September sea ice is reproduced more realistically by the simulations.

Overall, a substantial proportion of the literature relies on a single atmospheric reanalysis—most commonly ERA5—to infer mechanisms driving the 2023 Antarctic sea ice minimum. Our results demonstrate that the choice of atmospheric reanalysis can lead to markedly different regional sea ice responses, particularly during February 2023, with implications for the interpretation of both thermodynamic and dynamical drivers. Our study thus shows that caution should be taken when analysing real-world events from reanalysis-driven simulations, and the sensitivity of conclusions to the choice of atmospheric reanalysis should be assessed, and where possible multiple reanalysis products employed to improve the robustness of inferred mechanisms.

Code and data availability. Model outputs are available from lead author upon reasonable requests.

https://doi.org/10.5194/egusphere-2026-2719
Preprint. Discussion started: 27 May 2026

Author contributions. MG carried out the analysis and wrote the manuscript with input from AB and JA. AB and JA co-designed the study. AB provided lead supervision of MG. JA ran the model simulations and co-supervised MG.

Competing interests. The authors declare that they have no competing interests.

https://doi.org/10.5194/egusphere-2026-2719
Preprint. Discussion started: 27 May 2026

References

Abernathey, R. P., Cerovecki, I., Holland, P. R., Newsom, E., Mazloff, M., and Talley, L. D.: Water-mass transformation by sea ice in the upper branch of the Southern Ocean overturning, Nature Geoscience, 9, https://doi.org/10.1038/ngeo2749, num Pages: 8, 2016.

Alkama, R., Taylor, P. C., Garcia-San Martin, L., Douville, H., Duveiller, G., Forzieri, G., Swingedouw, D., and Cescatti, A.: Clouds damp the radiative impacts of polar sea ice loss, The Cryosphere, 14, 2673–2686, https://doi.org/10.5194/tc-14-2673-2020, 2020.

Aparício, S., Driscoll, S., and Flocco, D.: Observational data of Arctic Sea Ice Melt Ponds: a Systematic Review of Acquisition and Processing Approaches, https://doi.org/10.5194/egusphere-2025-4480, 2025.

Benestad, R. E., Mezghani, A., Lutz, J., Dobler, A., Parding, K. M., and Landgren, O. A.: Various ways of using empirical orthogonal functions for climate model evaluation, Geoscientific Model Development, 16, 2899–2913, https://doi.org/10.5194/gmd-16-2899-2023, 2023.

Blockley, E., Fiedler, E., Ridley, J., Roberts, L., West, A., Copsey, D., Feltham, D., Graham, T., Livings, D., Rousset, C., Schroeder, D., and Vancoppenolle, M.: The sea ice component of GC5: coupling SI^3 to HadGEM3 using conductive fluxes, Geoscientific Model Development, 17, 6799–6817, https://doi.org/10.5194/gmd-17-6799-2024, 2024.

Boehm, C. L., Thompson, D. W. J., and Blanchard-Wrigglesworth, E.: The key role of the Southern Annular Mode during the sea-ice maximum for Antarctic sea ice and its recent loss, Communications Earth & Environment, 6, 833, https://doi.org/10.1038/s43247-025-02792-2, 2025.

Bracegirdle, T. J. and Marshall, G. J.: The Reliability of Antarctic Tropospheric Pressure and Temperature in the Latest Global Reanalyses, Journal of Climate, 25, 7138–7146, 2012.

Bromwich, D. H., Fogt, R. L., Hodges, K. I., and Walsh, J. E.: A tropospheric assessment of the ERA-40, NCEP, and JRA-25 global reanalyses in the polar regions, Journal of Geophysical Research-Atmospheres, 112, D10 111, https://doi.org/10.1029/2006JD007859, 2007.

Bromwich, D. H., Nicolas, J. P., and Monaghan, A. J.: An Assessment of Precipitation Changes over Antarctica and the Southern Ocean since 1989 in Contemporary Global Reanalyses, Journal of Climate, 24, 4189–4209, https://doi.org/10.1175/2011JCLI4074.1, num Pages: 21 Web of Science ID: WOS:000294490600001, 2011.

Caton Harrison, T., Biri, S., Bracegirdle, T. J., King, J. C., Kent, E. C., Vignon, , and Turner, J.: Reanalysis representation of low-level winds in the Antarctic near-coastal region, Weather and Climate Dynamics, 3, 1415–1437, https://doi.org/10.5194/wcd-3-1415-2022, 2022.

Chan, A. C., England, M. R., Screen, J. A., Bracegirdle, T. J., Blockley, E. W., and Holmes, C. R.: Extreme Antarctic Sea Ice Loss Facilitated by Negative Shift of Southern Annular Mode, Geophysical Research Letters, 52, e2025GL116 688, https://doi.org/10.1029/2025GL116688, _eprint: https://agupubs.onlinelibrary.wiley.com/doi/pdf/10.1029/2025GL116688, 2025.

Comiso, J. C.: Bootstrap Sea Ice Concentrations from Nimbus-7 SMMR and DMSP SSM/I-SSMIS, Version 4 [Data Set], NASA NSIDC Distributed Active Archive Center, https://doi.org/10.5067/X5LG68MH013O, 2023.

Comiso, J. C., Cavalieri, D. J., Parkinson, C. L., and Gloersen, P.: Passive microwave algorithms for sea ice concentration: A comparison of two techniques, Remote Sensing of Environment, 60, 357–384, https://doi.org/10.1016/S0034-4257(96)00220-9, 1997.

de Azevedo, H. B., Casagrande, F., and Allende, S.: Analysis of the Unprecedented Reduction in Antarctic Sea Ice During the Years 2022–2023, International Journal of Climatology, 45, e70 147, https://doi.org/10.1002/joc.70147, _eprint: https://rmets.onlinelibrary.wiley.com/doi/pdf/10.1002/joc.70147, 2025.

Diamond, R., Sime, L. C., Holmes, C. R., and Schroeder, D.: CMIP6 Models Rarely Simulate Antarctic Winter Sea-Ice Anomalies as Large as Observed in 2023, Geophysical Research Letters, 51, e2024GL109 265, https://doi.org/10.1029/2024GL109265, _eprint: https://agupubs.onlinelibrary.wiley.com/doi/pdf/10.1029/2024GL109265, 2024.

DiGirolamo, N. E., Parkinson, C. L., Cavalieri, D. J., Gloersen, P., and Zwally, H. J.: Sea ice concentrations from Nimbus-7 SMMR and DMSP SSM/I-SSMIS passive microwave data, (NSIDC-0051, Version 2) [Data Set], NASA NSIDC Distributed Active Archive Center, https://doi.org/10.5067/MPYG15WAA4WX, 2022.

Dou, J. and Zhang, R.: Combined Influences of Atmospheric Precursors on Antarctic Sea Ice and Its Record Low in February 2023, Advances in Atmospheric Sciences, 42, 2435–2452, https://doi.org/10.1007/s00376-025-4309-9, 2025.

Eabry, M. D., Goyal, R., Taschetto, A. S., Hobbs, W., and Gupta, A. S.: Combined Impacts of Southern Annular Mode and Zonal Wave 3 on Antarctic Sea Ice Variability, Journal of Climate, 37, 1759–1775, https://doi.org/10.1175/JCLI-D-23-0516.1, 2024.

Espinosa, Z. I., Blanchard-Wrigglesworth, E., and Bitz, C. M.: Understanding the drivers and predictability of record low Antarctic sea ice in austral winter 2023, Communications Earth & Environment, 5, 723, https://doi.org/10.1038/s43247-024-01772-2, 2024.

Feng, J., Zhang, Y., Cheng, Q., Liang, X. S., and Jiang, T.: Analysis of summer Antarctic sea ice anomalies associated with the spring Indian Ocean dipole, Global and Planetary Change, 181, 102 982, https://doi.org/10.1016/j.gloplacha.2019.102982, 2019.

Flocco, D., Schroeder, D., Feltham, D. L., and Hunke, E. C.: Impact of melt ponds on Arctic sea ice simulations from 1990 to 2007, Journal of Geophysical Research: Oceans, 117, https://doi.org/10.1029/2012JC008195, _eprint: https://agupubs.onlinelibrary.wiley.com/doi/pdf/10.1029/2012JC008195, 2012.

Fretwell, P. T., Boutet, A., and Ratcliffe, N.: Record low 2022 Antarctic sea ice led to catastrophic breeding failure of emperor penguins, Communications Earth & Environment, 4, 273, https://doi.org/10.1038/s43247-023-00927-x, 2023.

Goosse, H., Libera, S., Naveira Garabato, A. C., Richaud, B., Silvano, A., and Vancoppenolle, M.: Winter sea ice edge shaped by Antarctic Circumpolar Current pathways, The Cryosphere, 19, 5763–5779, https://doi.org/10.5194/tc-19-5763-2025, 2025.

Griffies, S.: OMIP contribution to CMIP6: experimental and diagnostic protocol for the physical component of the Ocean Model Intercomparison Project, EGU, 2016.

Hersbach, H., Bell, B., Berrisford, P., Hirahara, S., Horányi, A., Muñoz-Sabater, J., Nicolas, J., Peubey, C., Radu, R., Schepers, D., Simmons, A., Soci, C., Abdalla, S., Abellan, X., Balsamo, G., Bechtold, P., Biavati, G., Bidlot, J., Bonavita, M., De Chiara, G., Dahlgren, P., Dee, D., Diamantakis, M., Dragani, R., Flemming, J., Forbes, R., Fuentes, M., Geer, A., Haimberger, L., Healy, S., Hogan, R. J., Hólm, E., Janisková, M., Keeley, S., Laloyaux, P., Lopez, P., Lupu, C., Radnoti, G., de Rosnay, P., Rozum, I., Vamborg, F., Villaume, S., and Thépaut, J.-N.: The ERA5 global reanalysis, Quarterly Journal of the Royal Meteorological Society, 146, 1999–2049, https://doi.org/10.1002/qj.3803, _eprint: https://rmets.onlinelibrary.wiley.com/doi/pdf/10.1002/qj.3803, 2020.

Hobbs, W. R., Massom, R., Stammerjohn, S., Reid, P., Williams, G., and Meier, W.: A review of recent changes in Southern Ocean sea ice, their drivers and forcings, Global and Planetary Change, 143, 228–250, https://doi.org/10.1016/j.gloplacha.2016.06.008, 2016.

Hobbs, W. R., Spence, P., Meyer, A., et al.: Observational evidence for a regime shift in summer Antarctic sea ice, Journal of Climate, 37, 2263–2275, https://doi.org/10.1175/JCLI-D-23-0479.1, 2024.

Jena, B., Kshitija, S., Bajish, C. C., Turner, J., Holmes, C., Wilkinson, J., Mohan, R., and Thamban, M.: Evolution of Antarctic Sea Ice Ahead of the Record Low Annual Maximum Extent in September 2023, Geophysical Research Letters, 51, e2023GL107 561, https://doi.org/10.1029/2023GL107561, _eprint: https://agupubs.onlinelibrary.wiley.com/doi/pdf/10.1029/2023GL107561, 2024.

https://doi.org/10.5194/egusphere-2026-2719
Preprint. Discussion started: 27 May 2026

Jones, R. W., Renfrew, I. A., Orr, A., Webber, B. G. M., Holland, D. M., and Lazzara, M. A.: Evaluation of four global reanalysis products using in situ observations in the Amundsen Sea Embayment, Antarctica, Journal of Geophysical Research: Atmospheres, 121, 6240–6257, https://doi.org/10.1002/2015JD024680, _eprint: https://agupubs.onlinelibrary.wiley.com/doi/pdf/10.1002/2015JD024680, 2016.

Josey, S. A., Meijers, A. J. S., Blaker, A. T., Grist, J. P., Mecking, J., and Ayres, H. C.: Record-low Antarctic sea ice in 2023 increased ocean heat loss and storms, Nature, 636, 635–639, https://doi.org/10.1038/s41586-024-08368-y, 2024.

Kobayashi, Shinya and National Center for Atmospheric Research Staff: The Climate Data Guide: JRA-55, https://climatedataguide.ucar.edu/climate-data/jra-55, 2025.

Kurtz, N. T. and Markus, T.: Satellite observations of Antarctic sea ice thickness and volume, Journal of Geophysical Research: Oceans, 117, https://doi.org/10.1029/2012JC008141, 2012.

Kusahara, K. and Tatebe, H.: Causes of the Abrupt and Sustained 2016–2023 Antarctic Sea-Ice Decline: A Sea Ice–Ocean Model Perspective, Geophysical Research Letters, 52, e2025GL115 256, https://doi.org/10.1029/2025GL115256, _eprint: https://agupubs.onlinelibrary.wiley.com/doi/pdf/10.1029/2025GL115256, 2025.

Lenaerts, J. T. M., Van Tricht, K., Lhermitte, S., and L'Ecuyer, T. S.: Polar clouds and radiation in satellite observations, reanalyses, and climate models, Geophysical Research Letters, 44, 3355–3364, https://doi.org/10.1002/2016GL072242, _eprint: https://agupubs.onlinelibrary.wiley.com/doi/pdf/10.1002/2016GL072242, 2017.

Liu, Y., Sun, C., Li, J., Kucharski, F., Di Lorenzo, E., Abid, M. A., and Li, X.: Decadal oscillation provides skillful multiyear predictions of Antarctic sea ice, Nature Communications, 14, 961, https://doi.org/10.1038/s41467-023-44094-1, 2023.

Lorenz, E. N.: Empirical orthogonal functions and statistical weather prediction, Scientific Report No. 1, Statistical Forecasting Project, 1956.

Ma, W., Li, X., Zhang, L., Hou, Y., and Man, K.: Sea Ice Dipole Around East Antarctica Induced by Remote Forcing From Indian Ocean, Journal of Geophysical Research: Atmospheres, 130, e2024JD042 435, https://doi.org/10.1029/2024JD042435, _eprint: https://agupubs.onlinelibrary.wiley.com/doi/pdf/10.1029/2024JD042435, 2025.

Madec, G. and NEMO System Team: NEMO Ocean Engine Reference Manual, Zenodo, doi:10.5281/zenodo.1464816, 2024.

Massom, R. A., Scambos, T. A., Bennetts, L. G., Reid, P., Squire, V. A., and Stammerjohn, S. E.: Antarctic ice shelf disintegration triggered by sea ice loss and ocean swell, Nature, 558, 383–389, https://doi.org/10.1038/s41586-018-0212-1, 2018.

Massonnet, F., Fichefet, T., Goosse, H., Bitz, C. M., Philippon-Berthier, G., Holland, M. M., and Barriat, P.-Y.: Constraining projections of summer Arctic sea ice, The Cryosphere, 6, 1383–1394, https://doi.org/10.5194/tc-6-1383-2012, 2012.

Mayer, J., Mayer, M., and Haimberger, L.: Consistency and Homogeneity of Atmospheric Energy, Moisture, and Mass Budgets in ERA5, Journal of Climate, 34, 3955–3974, https://doi.org/10.1175/JCLI-D-20-0676.1, 2021.

Maykut, G. A. and Perovich, D. K.: The role of shortwave radiation in the summer decay of a sea ice cover, Journal of Geophysical Research: Oceans, 92, 7032–7044, https://doi.org/10.1029/JC092iC07p07032, _eprint: https://agupubs.onlinelibrary.wiley.com/doi/pdf/10.1029/JC092iC07p07032, 1987.

Mezzina, B., Goosse, H., Huot, P.-V., Marchi, S., and Van Lipzig, N.: Contributions of atmospheric forcing and ocean preconditioning in the 2016 Antarctic sea ice extent drop, ENVIRONMENTAL RESEARCH-CLIMATE, 3, https://doi.org/10.1088/2752-5295/ad3a0b, 2024.

National Snow and Ice Data Center: Antarctic Sea Ice Minimum Hits a Near-Record Low, Again, https://nsidc.org/sea-ice-today/analyses/antarctic-sea-ice-minimum-hits-near-record-low-again, 2025.

https://doi.org/10.5194/egusphere-2026-2719
Preprint. Discussion started: 27 May 2026

National Snow and Ice Data Center: Descriptions of and Differences Between the NASA Team and Bootstrap Algorithms, https://nsidc.org/data/user-resources/help-center/descriptions-and-differences-between-nasa-team-and-bootstrap-algorithms, accessed: 2026-03-17, 2026.

Notz, D. and Marotzke, J.: Observations reveal external driver for Arctic sea-ice retreat, Geophysical Research Letters, 39, https://doi.org/10.1029/2012GL051094, _eprint: https://agupubs.onlinelibrary.wiley.com/doi/pdf/10.1029/2012GL051094, 2012.

Orr, A., Lu, H., Martineau, P., Gerber, E. P., Marshall, G. J., and Bracegirdle, T. J.: Is our dynamical understanding of the circulation changes associated with the Antarctic ozone hole sensitive to the choice of reanalysis dataset?, Atmospheric Chemistry and Physics, 21, 7451–7472, https://doi.org/10.5194/acp-21-7451-2021, 2021.

Palerme, C., Claud, C., Dufour, A., Genthon, C., Wood, N. B., and L'Ecuyer, T.: Evaluation of Antarctic snowfall in global meteorological reanalyses, Atmospheric Research, 190, 104–112, https://doi.org/10.1016/j.atmosres.2017.02.015, 2017.

Purich, A. and Doddridge, E. W.: Record low Antarctic sea ice coverage indicates a new sea ice state, Communications Earth & Environment, 4, 314, https://doi.org/10.1038/s43247-023-00961-9, 2023.

Raphael, M. N., Maierhofer, T. J., Fogt, R. L., Hobbs, W. R., and Handcock, M. S.: A twenty-first century structural change in Antarctica's sea ice system, Communications Earth & Environment, 6, 131, https://doi.org/10.1038/s43247-025-02107-5, num Pages: 9 Web of Science ID: WOS:001427684000004, 2025.

Renwick, J. A., Kohout, A., and Dean, S.: Atmospheric Forcing of Antarctic Sea Ice on Intraseasonal Time Scales, Journal of Climate, 25, 5962–5975, https://doi.org/10.1175/JCLI-D-11-00423.1, 2012.

Richaud, B., Massonnet, F., Fichefet, T., Topál, D., Barthélemy, A., and Docquier, D.: Anatomy of Arctic and Antarctic sea ice lows in an ocean–sea ice model, The Cryosphere, 20, 791–810, https://doi.org/10.5194/tc-20-791-2026, 2026.

Schroeter, S., O'Kane, T. J., and Sandery, P. A.: Antarctic sea ice regime shift associated with decreasing zonal symmetry in the Southern Annular Mode, The Cryosphere, 17, 701–717, https://doi.org/10.5194/tc-17-701-2023, 2023.

Serreze, M. C. and Meier, W. N.: The Arctic's sea ice cover: trends, variability, predictability, and comparisons to the Antarctic, https://doi.org/10.1111/nyas.13856, iSSN: 1 Volume: 1436, 2018.

Silber, I., Verlinde, J., Wang, S.-H., Bromwich, D. H., Fridlind, A. M., Cadeddu, M., Eloranta, E. W., and Flynn, C. J.: Cloud Influence on ERA5 and AMPS Surface Downwelling Longwave Radiation Biases in West Antarctica, Journal of Climate, 32, 7935–7949, https://doi.org/10.1175/JCLI-D-19-0149.1, 2019.

Singarayer, J. S. and Bamber, J. L.: EOF analysis of three records of sea-ice concentration spanning the last 30 years, Geophysical Research Letters, 30, 1251, https://doi.org/10.1029/2002GL016640, 2003.

Spira, T., du Plessis, M., Haumann, F. A., Giddy, I., Narayanan, A., Silvano, A., and Swart, S.: Wind-triggered Antarctic sea-ice decline preconditioned by thinning Winter Water, Nature Climate Change, pp. 1–8, https://doi.org/10.1038/s41558-026-02601-4, 2026.

Stroeve, J. C., Kattsov, V., Barrett, A., Serreze, M., Pavlova, T., Holland, M., and Meier, W. N.: Trends in Arctic sea ice extent from CMIP5, CMIP3 and observations, Geophysical Research Letters, 39, https://doi.org/10.1029/2012GL052676, _eprint: https://agupubs.onlinelibrary.wiley.com/doi/pdf/10.1029/2012GL052676, 2012a.

Stroeve, J. C., Serreze, M. C., Holland, M. M., Kay, J. E., Malanik, J., and Barrett, A. P.: The Arctic's rapidly shrinking sea ice cover: a research synthesis, Climatic Change, 110, 1005–1027, https://doi.org/10.1007/s10584-011-0101-1, 2012b.

Swathi, M., Kumar, A., Yadav, J., and Mohan, R.: The role of atmospheric and oceanic factors on the record low Antarctic sea ice extent of 2023, Global and Planetary Change, 252, 104 858, https://doi.org/10.1016/j.gloplacha.2025.104858, 2025.

https://doi.org/10.5194/egusphere-2026-2719
Preprint. Discussion started: 27 May 2026

Tetzner, D., Thomas, E., and Allen, C.: A Validation of ERA5 Reanalysis Data in the Southern Antarctic Peninsula—Ellsworth Land Region, and Its Implications for Ice Core Studies, Geosciences, 9, https://doi.org/10.3390/geosciences9070289, 2019.

Tian, T., Yang, S., Høyer, J. L., Nielsen-Englyst, P., and Singha, S.: Cooler Arctic surface temperatures simulated by climate models are closer to satellite-based data than the ERA5 reanalysis, Communications Earth & Environment, 5, 111, https://doi.org/10.1038/s43247-024-01276-z, 2024.

Tsamados, M., Feltham, D. L., Schroeder, D., Flocco, D., Farrell, S. L., Kurtz, N., Laxon, S. W., and Bacon, S.: Impact of Variable Atmospheric and Oceanic Form Drag on Simulations of Arctic Sea Ice, Journal of Physical Oceanography, https://doi.org/10.1175/JPO-D-13-0215.1, 2014.

Tsujino, H., Urakawa, S., Nakano, H., Small, R. J., Kim, W. M., Yeager, S. G., Danabasoglu, G., Suzuki, T., Bamber, J. L., Bentsen, M., Böning, C. W., Bozec, A., Chassignet, E. P., Curchitser, E., Boeira Dias, F., Durack, P. J., Griffies, S. M., Harada, Y., Ilicak, M., Josey, S. A., Kobayashi, C., Kobayashi, S., Komuro, Y., Large, W. G., Le Sommer, J., Marsland, S. J., Masina, S., Scheinert, M., Tomita, H., Valdivieso, M., and Yamazaki, D.: JRA-55 based surface dataset for driving ocean–sea-ice models (JRA55-do), Ocean Modelling, 130, 79–139, https://www.sciencedirect.com/science/article/pii/S146350031830235X, 2018.

Vancoppenolle, M., Rousset, C., Blockley, E., Aksenov, Y., Feltham, D., Garric, G., Guémas, V., Iovino, D., Keeley, S., Madec, G., Massonnet, F., Ridley, J., Schroeder, D., and Tietsche, S.: SI3, the NEMO Sea Ice Engine, https://doi.org/10.5281/zenodo.7534900, 2023.

von Storch, H. and Zwiers, F. W.: Statistical Analysis in Climate Research, Cambridge University Press, Cambridge, UK, 1999.

Wang, J., Massonnet, F., Goosse, H., Luo, H., Barthélemy, A., and Yang, Q.: Synergistic atmosphere-ocean-ice influences have driven the 2023 all-time Antarctic sea-ice record low, Communications Earth & Environment, 5, 415, https://doi.org/10.1038/s43247-024-01523-3, 2024a.

Wang, S., Liu, J., Cai, W., Yang, D., Kerzenmacher, T., Ding, S., and Cheng, X.: Strong impact of the rare three-year La Niña event on Antarctic surface climate changes in 2021–2023, npj Climate and Atmospheric Science, 8, 173, https://doi.org/10.1038/s41612-025-01066-0, 2025.

Wang, Y., Zhou, D., Bunde, A., and Havlin, S.: Testing reanalysis data sets in Antarctica: Trends, persistence properties, and trend significance, Journal of Geophysical Research: Atmospheres, 121, 12,839–12,855, https://doi.org/10.1002/2016JD024864, _eprint: https://agupubs.onlinelibrary.wiley.com/doi/pdf/10.1002/2016JD024864, 2016.

Wang, Z., Fraser, A. D., Reid, P., O'Farrell, S., and Coleman, R.: Antarctic sea ice surface temperature bias in atmospheric reanalyses induced by the combined effects of sea ice and clouds, Communications Earth & Environment, 5, 552, https://doi.org/10.1038/s43247-024-01692-1, 2024b.

Wu, Q., Ma, Y., Hu, A., Rosenbloom, N., Zhang, L., Liu, H., Liu, S., Yang, L., and Yang, C.: Pacific sub-decadal sea surface temperature variations contributed to recent Antarctic Sea ice decline trend, Nature Communications, 16, 3386, https://doi.org/10.1038/s41467-025-58788-1, 2025.

Yuan, X. and Martinson, D. G.: The Antarctic dipole and its predictability, Journal of Climate, 14, 4597–4613, https://doi.org/10.1175/1520-0442(2001)014<4597:TADAPI>2.0.CO;2, 2001.